Available online at www.sciencedirect.com

SciVerse ScienceDirect

journal homepage: www.elsevier.com/locate/he

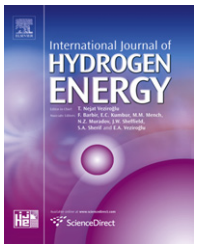

Improving the performance of a spark-ignited gasoline engine with the addition of syngas produced by onboard ethanol steaming reforming

Changwei Ji, Xiaoxu Dai, Bingjie Ju, Shuofeng Wang, Bo Zhang, Chen Liang, Xiaolong Liu*

College of Environmental and Energy Engineering, Beijing University of Technology, Beijing 100124, PR China

ARTICLE INFO

Article history:
Received 14 December 2011
Received in revised form
21 January 2012
Accepted 31 January 2012
Available online 8 March 2012

Keywords:
Syngas
Steam reforming
Exhaust heat recovery
Combustion
Emissions
Spark-ignited engines

ABSTRACT

Producing the syngas by onboard ethanol steam reforming is an effective way for recovering the exhaust heat in the engine tailpipe. Besides, as hydrogen is contained in the syngas, the addition of syngas is also capable of improving engine combustion and emissions characteristics. In this paper, an experimental study was carried out on a four-cylinder 1.6 L spark-ignited engine to explore the effect of syngas addition on the engine performance. A fuel reforming reactor with the copper based catalysts was designed and mounted on the engine tailpipe, so that the ethanol solution could be decomposed to be syngas which is mainly composed of hydrogen and carbon monoxide when the catalysts were heated by the exhaust gas. The intake manifolds was also modified to permit syngas to be injected into the fourth cylinder of the engine. The engine was run at 1800 rpm and a manifolds absolute pressure of 61.5 kPa. The spark timing for the maximum brake torque was adopted for each testing point. The syngas volume fraction in the total intake gas was gradually increased from 0% to 2.43%. Meanwhile, the gasoline injection duration governing by a hybrid electronic control unit was adjusted to keep the excess air ratio of the fuel-air mixture in the fourth cylinder at about 1.00. The experimental results demonstrated that the syngas volume flow rate was markedly enhanced from 90 to 240 L/h when the feedstock flow rate was increased from 18 to 54 mL/min. The peak ethanol conversion efficiency reached 81.16% at a feedstock flow rate of 36 mL/min. The hydrogen concentration was increased whereas carbon monoxide concentration was decreased in the syngas with the increase of the feedstock supply. The engine indicated thermal efficiency was raised to be 39.01% at the syngas volume fraction of 2.43%. The flame development and propagation durations were shortened; HC and NOx emissions were reduced whereas CO emission was increased after the syngas addition at the stoichiometric condition.

1. Introduction

The limited fossil fuel reserves and adversely increased environmental pollution have pushed investigations on searching new and clean alternative fuels for internal combustion (IC) engines. Hydrogen has been proposed to be a kind of promising energy source for spark-ignited (SI) engines [1–11]. Generally, the low ignition energy, high flame and diffusion speed of hydrogen contribute to the improved engine performance [12–19]. However, since the energy

* *Corresponding author*. Tel./fax: +86 1067392126.
E-mail address: chwji@bjut.edu.cn (C. Ji).
0360-3199/$ – see front matter
doi:10.1016/j.ijhydene.2012.01.153

density of hydrogen on volume basis is much lower than that of gasoline, hydrogen engines are prone to produce a lower power output than gasoline engines [20].

Compared with the pure hydrogen-fueled engines, using small amount of hydrogen as an additive to gasoline engines can not only reduce the engine fuel consumption and toxic emissions, but also ensure the power output at part load conditions [21–24]. Ji et al. [25–27] carried out a series of experiments on an SI engine to investigate the effect of hydrogen addition on improving the gasoline engine performance under various conditions. It was found that the engine thermal efficiency and emissions performance were improved with the increase of hydrogen addition level. The flame development and propagation durations and cyclic variation were reduced with hydrogen enrichment at lean conditions. Wang et al. [28] investigated the effect of hydrogen addition fraction on the combustion and emissions characteristics of a spark-ignited ethanol engine. The test results showed that hydrogen addition was effective on reducing the cyclic variation and improving indicated thermal efficiency of the ethanol engine at idle and stoichiometric conditions. Furthermore, the acetaldehyde emission was also reduced with the increase of hydrogen addition fraction. Li et al. [29] studied the mechanism of toxic emissions formation process in the engine fueled with hydrogen-gasoline mixtures. He got the conclusion that NOx, HC and CO emissions from the hydrogen-enriched gasoline engine were lower than those of the original engine. Unfortunately, although hydrogen addition could improve the engine combustion and emissions performance, the limited hydrogen infrastructure distribution and risks in hydrogen storage and transportation are still barriers for the commercialization of hydrogen-blended engines [30,31].

The onboard hydrogen production by fuel reforming provides a feasible solution for the application of hydrogen on vehicles [32,33]. Generally, only one-third of the energy provided by the fuel could be used to drive the vehicle, and about 36%–50% energy provided by the fuel is directly expelled through the tailpipe [34–37]. Therefore, the exhaust heat recovery could be seen as an effective way for enhancing the engine overall efficiency. At present, the steam reforming (SR) is one of the most widely used thermochemical processes for hydrogen production, which can liberate the maximum quantity of hydrogen. Due to the high hydrogen production yield and low rate of side reactions and by-products, the SR of hydrocarbons is regarded as a feasible method to provide the syngas (H_2, CO and ethanol etc.) which can be used to improve the engine performance [38]. The properties of hydrogen, carbon monoxide along with gasoline are listed in Table 1. The feedstocks of SR currently include alcohols, liquid hydrocarbons, ethers, gasoline and diesel. Methanol is one of the most commonly used feedstocks for SR, because the reaction could be easily processed at low temperatures [39]. But the high toxicity of methanol brings risks to human health. Ethanol is considered to be another good feedstock for producing hydrogen. Compared with other hydrocarbons, ethanol is a kind of renewable materials, which can be easily derived from biomass. Besides, ethanol also gains other good properties, such as easy transport, biodegradability and low toxicity [40–42]. Yang et al. [43] studied the steam reforming of ethanol (SRE) over Ni/ZnO catalysts to produce hydrogen. The results showed that ZnO is a promising support for preparing the nickel based reforming catalysts. Both increasing the molar ratio of water to ethanol within the range of 3–12 and raising the Ni loading within the range of 5 wt % to 20 wt % availed improving the H_2 concentration and suppressing the CH_4 formation. Steam reforming of methanol (SRM) to produce hydrogen over $CuO/ZnO/CeO_2/ZrO_2/Al_2O_3$ catalysts was studied by Huang et al. [44]. He found that CeO_2, ZrO_2 and Al_2O_3 benefited improving the dispersions of CuO and ZnO in $CuO/ZnO/CeO_2/ZrO_2/Al_2O_3$ catalysts. ZnO promoted the SRM reactions and slightly reduced the concentration of CO. But CeO_2 and Al_2O_3 weakened the SRM reactions. Nevertheless, the appropriate amount of Al_2O_3 was necessary for enhancing the stability and mechanical strength of the catalysts. Cheolwoong et al. [45] studied the performance of an SI engine fueled with the gasoline and ethanol-syngas. The test results demonstrated that the addition of simulated syngas could enhance the combustion stability. Moreover, HC and NOx emissions were reduced with the introduction of simulated syngas.

However, although many papers have investigated the effect of hydrogen addition on the engine performance and hydrogen production by the SR reactions with different catalysts, there are few published papers focusing on the onboard producing of the syngas with waste heat recovery and feeding the engine with the blends of gasoline and on-line produced syngas. In this study, an experiment was conducted to investigate the effect of syngas addition on the combustion and emissions characteristics of a gasoline engine. A self-designed fuel reforming reactor with the copper based catalysts was connected to the engine tailpipe, so that the feedstocks of SRE could be transformed into the syngas when the catalysts were heated by the exhaust gas. The syngas was injected into the fourth cylinder of the engine. The exhaust gas temperature generally has significant effect on the products of the reforming process. To enable the copper based catalysts to work at relatively high temperatures, the test was conducted at an engine speed of 1800 rpm and a manifolds absolute pressure (MAP) of 61.5 kPa. The syngas volume fraction in the total intake gas was increased from 0% to 2.43% to investigate the effect of syngas enrichment on the engine

Table 1 – Properties of gasoline, hydrogen and carbon monoxide.

Properties	Hydrogen	Carbon monoxide	Gasoline
Molecular weight (g/mol)	2.02	28.01	110
Specific heat (kJ/kg.K)	1.44	1.05	1.7
Stoichiometric fuel to air ratio (F/A)	34.3	2.5	14.6
Minimum ignition energy (mJ)	0.02	0.23	0.24
Ignition temperature (K)	858	913	530
Flame speed at 20 °C (cm/s)	237	126	41.5
Limits of flammability (vol% in air)	4.1–75	12.5–74.6	1.5–7.6
Lower heating value (MJ/kg)	120	10.01	44

thermal efficiency, combustion and emissions performance under the stoichiometric condition.

2. Experimental setup and procedure

2.1. Experimental setup

2.1.1. Catalyst samples

Copper and nickel are widely used as non-noble metal catalysts, which show better performance in SR for hydrogen production than others. Moreover, the low costs also make copper and nickel to be more promising for practical use than noble metal catalysts. In this study, the copper based catalysts are coated to the ceramic spherical body (diameter: 5.0 ± 0.5 mm). And the copper based catalyst sample is prepared by impregnating a γ-Al_2O_3 carrier, with an aqueous solution of $Cu(NO_3)_2 \cdot 3H_2O$, $Zn(NO_3)_2 \cdot 6H_2O$, $Al(NO_3)_3 \cdot 9H_2O$ and $Zr(NO_3)_4 \cdot 5H_2O$, followed by exsiccation at 110 °C for 2 h and calcination at 500 °C for 4 h. The γ-Al_2O_3 carrier is obtained by impregnating $\alpha.Al_2O_3.nH_2O$, $Ba(NO_3)_2$, $La(NO_3)_3.6H_2O$ and $Ce(NO_3)_3.6H_2O$ with an aqueous deionized water which is kept being vigorously stirred, followed by exsiccation at 110 °C for 24 h and calcination at 500 °C for 4 h.

2.1.2. Fuel reforming reactor

The fuel reforming reactor is designed to recover the exhaust heat for the catalysts and SR reactions. The reactor is connected to the end of three-way catalytic converter. The engine exhaust gas flows through nine stainless heat pipes (long: 298 mm, internal diameter: 28 mm) which are placed inside the reactor to get and transport the heat, so that the catalysts and feedstocks can be heated by the exhaust heat in the heat pipes. When the reactor is heated, the feedstocks are firstly transformed from the liquid phase into gaseous phase. Then, the gaseous feedstocks could be further converted into the syngas with the effect of catalysts. The volume of catalysts filled in the reactor is about 2.35 L. Since the exhaust gas temperature is very important to the catalysts activity, two temperature transducers are placed on the anterior and posterior parts of the reactor to monitor the exhaust temperature, respectively. The feedstocks of SR are ethanol and deionized water, and the water/ethanol molar ratio is 3:1 which is close to the stoichiometric equivalence ratio. A pump and a flow rate controller are adopted to adjust the flow rate of feedstocks into the reactor. As the unreacted feedstocks in SRE are unexpected in the products, a cold-trap and a pressure stabilizing vessel with desiccant are applied to purify the syngas. The syngas volume flow rate is monitored by a flow meter, and the syngas is sampled by a gas sampling pipe. A gas chromatograph (GC) equipped with a thermal conduct detector (TCD) is used to analyze the concentration of each component in the sample. A one-way valve is adopted to prevent refluxing of the syngas.

2.1.3. Engine testing system

The engine used in this experiment is a 1.6 L, four-cylinder, SI engine manufactured by Beijing Hyundai Motors. Table 2 displays the detailed specifications of the test engine. The schematic diagram of the experimental system is shown in Fig. 1. The syngas is introduced into the intake manifold of the fourth cylinder. A hybrid electronic control unit (HECU) which communicates with the engine original electronic control unit (OECU) and a calibration computer is used to govern the spark timings, injection timing and duration of the gasoline. A GW 160 eddy current dynamometer is coupled with engine to control the engine speed by automatically adjusting the load applied on the engine crankshaft (measurement deviation: <±1 rpm). The gasoline flow rate is determined by a FC2210 gasoline mass flow meter (measurement uncertainty: <±0.4 g/min). The air mass flow rate is monitored by a 20N060 thermal mass flow meter (measurement uncertainties: <±0.1 L/min). The in-cylinder pressure data acquisition and combustion analysis system consists of a Kistler 2613B optical encoder (crank angle resolution: 0.2 °CA, measurement deviation: <±0.01 °CA), a Kistler 6117BCD17 cylinder pressure transducer with a spark plug (measurement uncertainty: <±0.3 bar) and a Dewetron combustion analyzer. The cylinder pressure transducer is screwed into the cylinder head of the fourth cylinder to acquire the combustion cylinder pressure and enforce ignition of the fourth cylinder. The exhaust emissions of NOx, HC and CO are measured by a Horiba MEXA-7100DEGR emissions analyzer. The measurement sensitivities are 0.01% for CO_2 emission, and 1 ppm for NOx, CO and HC emissions, respectively.

Table 2 – Engine specifications.

Engine manufacturer	Beijing HyunDAI manufacturer motors
Engine type	In-line, 4 stroke
Compression ratio	10:1
Bore/mm	77.4
Stroke/mm	85.0
Displacement/L	1.60
Rated Torque/(N m/rpm)	143.28/4500
Rated Power/(kW/rpm)	83.32/6000

2.2. Experimental procedure

The experiment was conducted after the engine was fully warmed up. During the test, the coolant and lubricant oil temperatures were kept around 85 ± 1 °C and 90 ± 1 °C, respectively. The engine speed was fixed at 1800 rpm. The main throttle was adjusted to ensure that the MAP was kept at 61.5 kPa for all testing points. The HECU was used to govern the engine spark timing and gasoline injection duration based on the sensor signals acquired from the OECU and commands from a calibration computer. The syngas volume fraction in the total intake gas (air and syngas) was gradually increased from 0% to 2.43% by raising the feedstock flow rate. The gasoline injection duration was reduced with the increase of syngas enrichment level to ensure the engine to be operated at the stoichiometric condition. The syngas volume fraction in the total intake gas (α) and the global excess air ratio (λ) are defined as:

$$\alpha = \dot{v}_s/(\dot{v}_s + \dot{v}_{air}) \quad (1)$$

$$\lambda = \dot{m}_{air}/(\dot{m}_g \cdot AF_{st,g} + \dot{m}_{H_2} \cdot AF_{st,H_2} + \dot{m}_{CO} \cdot AF_{st,CO}) \quad (2)$$

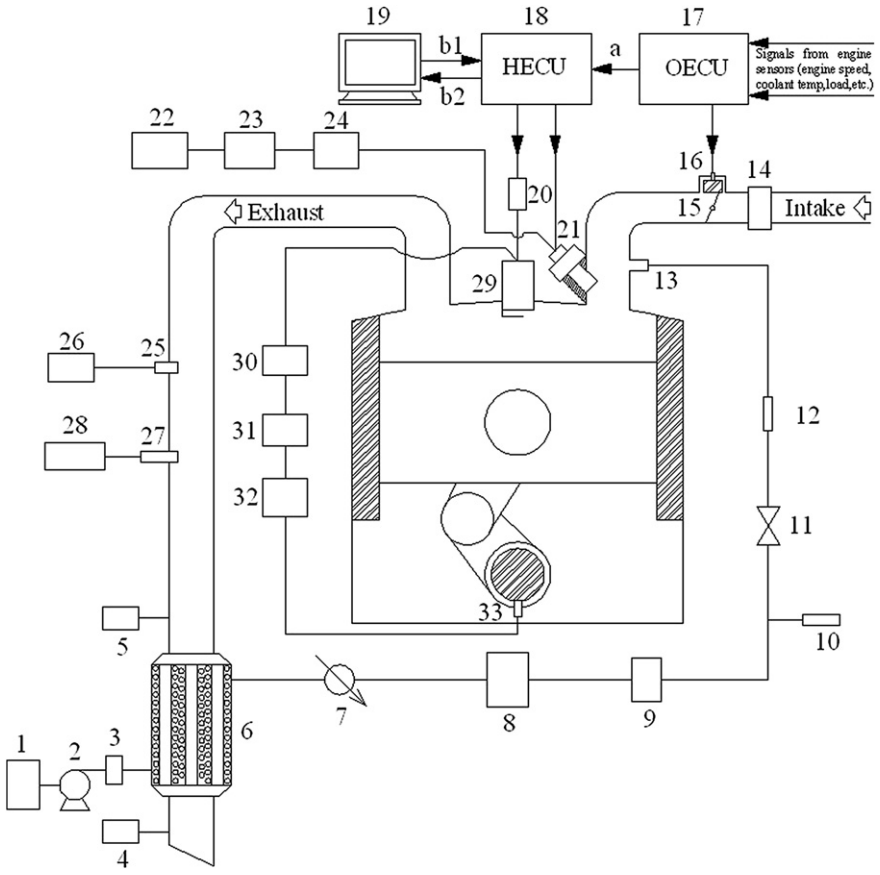

Fig. 1 – The schematics of the experiment system. 1. Feedstock tank; 2. Feedstock pump; 3. Feedstock flow meter; 4. Exhaust gas outtake temperature transducer; 5. Exhaust gas intake temperature transducer; 6. Reactor; 7. Cold-trap; 8. Pressure stabilizing vessel with desiccant; 9. Syngas flow meter; 10. Syngas sampling pipe; 11. Shutoff valve; 12. One-way valve; 13. Syngas intake pipe; 14. Air mass flow meter; 15. Throttle; 16. Idle valve; 17. Original ECU (OECU); 18. Hybrid electronic control unit ECU (HECU); 19. Calibration computer; 20. Ignition module; 21. Fuel injector; 22. Fuel tank; 23. Fuel mass flow meter; 24. Fuel pump; 25. O_2 sensor; 26. A/F analyzer; 27. Emissions sampling pipe; 28. MEXA-7100 emissions analyzer; 29. Pressure transducer with a spark plug; 30. Charge amplifier; 31. A/D converter; 32. Combustion analyzer; 33. Optical encoder; a. Signals from OECU to HECU; b1. Calibration and control signals from the calibration computer to HECU; b2. Data signals from HECU to a calibration PC.

In Eqs. (1) and (2), $\dot{v}_s$ and $\dot{v}_{air}$ are the measured volumetric flow rates of syngas and air at normal conditions (L/h), respectively; $\dot{m}_{air}$, $\dot{m}_g$, $\dot{m}_{H_2}$ and $\dot{m}_{CO}$ represent the measured air, gasoline, hydrogen and carbon monoxide mass flow rates (g/min); $AF_{st,g}$, AF_{st,H_2} and $AF_{st,CO}$ are the stoichiometric air-to-fuel ratios of gasoline, hydrogen and carbon monoxide ($AF_{st,g} = 14.6$ $AF_{st,H_2} = 34.3$ and $AF_{st,CO} = 2.5$).

The global excess air ratio was also monitored by a Horiba MEXA-110 A/F analyzer (measurement deviation: 0.1 A/F at A/F = 14.7) with an O_2 sensor inserted into the exhaust pipe of the fourth cylinder. The H/C molar ratio setting on the instrument was adjusted according to the measured gasoline, hydrogen and carbon monoxide mass flow rates, so that it can well measure the global excess air ratio of the IC engine. The deviation between the measured and calculated values was within ±5%. To investigate the engine performance under different syngas blending levels, the spark advance controlled by the HECU was adjusted to the maximum brake torque (MBT) spark timing for all testing points. Under each experimental condition, the in-cylinder pressure for 200 consecutive cycles were collected and analyzed through the Dewe-CA combustion analysis software to obtain the profiles of the indicated mean effective pressure, indicated thermal efficiency, CA0-10 and CA10-90 against syngas blending level, etc.

3. Results and discussion

3.1. *Ethanol steam reforming*

Fig. 2 depicts the variation of syngas flow rate with feedstock flow rate at 1800 rpm and a MAP of 61.5 kPa under stoichiometric condition. It can be found from Fig. 2 that the syngas flow rate is steadily increased with the increase of feedstock flow rate. The syngas flow rate is markedly raised from 90 to 240 L/h when the feedstock flow rate increases from 18 to 54 mL/min. Meanwhile, the increasing rate of syngas flow rate is slowly decreased when the feedstock flow rate exceeds

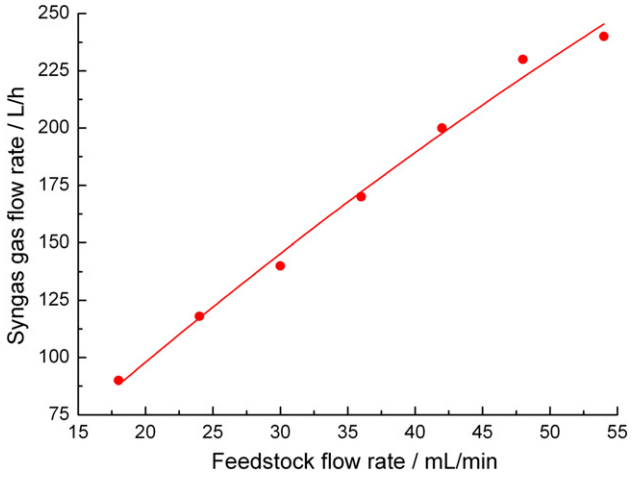

Fig. 2 – Syngas flow rate versus feedstock flow rate at 1800 rpm and a MAP of 61.5 kPa.

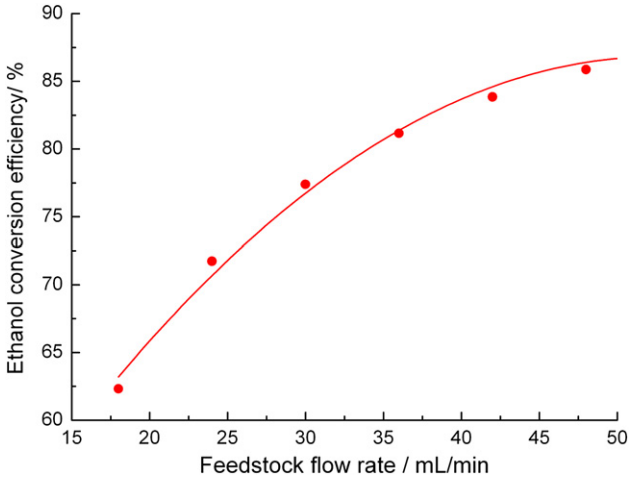

Fig. 4 – Ethanol conversion efficiency versus feedstock flow rate at 1800 rpm and a MAP of 61.5 kPa.

48 mL/min. The proper reason for this phenomenon can be ascribed to the fact that the excessive feedstocks could not be evaporated completely, due to the shortened evaporating time reserves. Moreover, the increasing rate of ethanol conversion efficiency is also decreased at high feedstock flow rates (see Fig. 4).

The main components of the syngas are hydrogen, carbon monoxide and small amounts of the unreacted feedstocks. Generally, the rates of hydrogen and carbon monoxide in the syngas directly reflect the quality of SRE. Fig. 3 shows the variations of hydrogen and carbon monoxide concentrations with feedstock flow rate at 1800 rpm and a MAP of 61.5 kPa. The hydrogen concentration increases from 50.64% to 59.65% when the feedstock flow rate increases from 18 to 54 mL/min. The possible reason is that the gas products and unreacted feedstocks after the reaction are easily to be removed from the reactor at the high reactor pressures and feedstock flow rates. Thereby, the surface of catalysts could be dried and cleaned with the properly increased feedstock flow rate. Besides, the

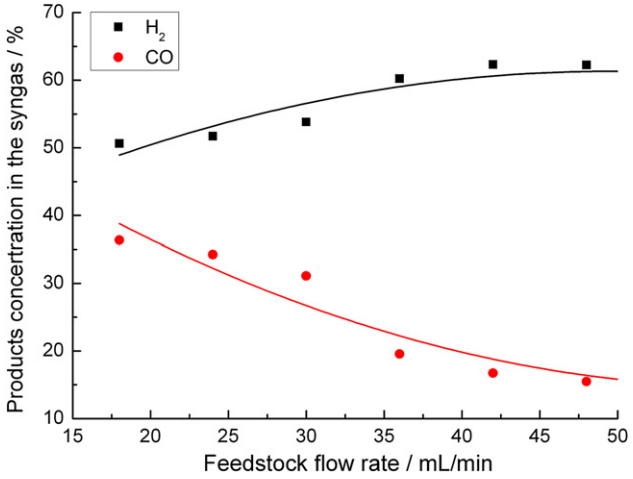

Fig. 3 – Products concentration in syngas versus feedstock flow rate at 1800 rpm and a MAP of 61.5 kPa.

increased H and OH radicals at high feedstock flow rates could also improve the hydrogen productivity [46]. Meanwhile, Fig. 3 also indicates that the carbon monoxide concentration decreases from 36.34% to 16.68% when the feedstock flow rate increases from 18 to 54 mL/min. The carbon monoxide formed during the reforming reaction can further react according to the water gas shift reaction (WGSR) [47].

$$CO + H_2O = CO_2 + H_2 \quad (3)$$

The water gas shift reaction can also take place as a secondary reaction to produce the additional hydrogen, due to the presences of carbon monoxide and excess water steam. Therefore, the hydrogen concentration varies in inverse proportion to the carbon monoxide concentration in the syngas.

The ethanol conversion efficiency is a key factor for evaluating the quality of SRE process. Fig. 4 displays the variation of ethanol conversion efficiency with feedstock flow rate at 1800 rpm and a MAP of 61.5 kPa. It can be seen from Fig. 4 that the ethanol conversion efficiency is improved with the increase of feedstock flow rate. The ethanol conversion efficiency rises from 62.32% to 81.16% when the feedstock flow rate increases from 18 to 36 mL/min. But the increasing rate of ethanol conversion efficiency is slightly depressed at high feedstock flow rates. This can be explained by the fact that as the SRE is a reversible process, the increased amount of feedstocks could promote the reaction in the positive direction and convert feedstocks into the syngas more efficiently. However, when the feedstocks are further added, the increasing rate of ethanol conversion efficiency tends to be reduced, due to the limited catalysts activity. Moreover, the excessive feedstocks would cost more energy in SRE, which hinders the conversion of ethanol.

3.2. *Indicated mean effective pressure and indicated thermal efficiency*

Indicated mean effective pressure (Imep) directly reflects the engine torque output. Fig. 5 shows the variations of Imep with

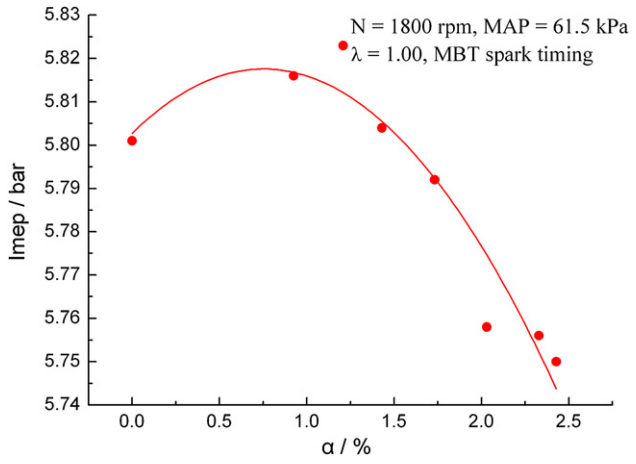

Fig. 5 – Indicated mean effective pressure versus the syngas volume fraction at 1800 rpm and a MAP of 61.5 kPa.

syngas volume fraction in the total intake gas at 1800 rpm and a MAP of 61.5 kPa. It can be found from Fig. 5 that Imep first increases and then decreases with the increase of syngas volume fraction. The low ignition energies and high flame speeds of hydrogen and carbon monoxide contribute to the enhanced combustion process. Besides, as the syngas is produced from the ethanol steam reforming, the ethanol may be introduced into the cylinder. As the ethanol possesses a relatively high latent heat, the evaporation of ethanol in the cylinder helps reduce the cylinder temperature, and therefore contributes to the elevated volumetric efficiency which benefits enhancing the engine power output. Therefore, Imep is slightly increased when the syngas volume fraction increases from 0% to 0.92%. But, since the energy densities hydrogen and carbon monoxide on volume basis are much lower than that of gasoline, the reduced fuel energy flow rate is attained after the syngas addition, which finally results in the dropped Imep at high syngas volume fractions in the intake gas.

The engine indicated thermal efficiency is crucial for evaluating the engine fuel economy, which can be improved by either optimizing the combustion system or improving the fuel combustion properties. Fig. 6 shows the variation of engine indicated thermal efficiency with the syngas volume fraction. As it is seen from Fig. 6, the engine indicated thermal efficiency is markedly enhanced from 34.52% of the original engine to 39.01% of the 2.43% syngas-blended gasoline engine. The possible interpretation could be attributed to the fact that the syngas-gasoline mixtures could be burnt more completely than the pure gasoline due to the wide flammability of hydrogen and carbon monoxide. Besides, the shortened flame development and propagation periods after the syngas addition (see Figs. 7 and 8) also symbolize the reduced cooling and exhaust losses which contribute to the improved indicated thermal efficiency. Meanwhile, the short quenching distance of hydrogen also enables the flame of the syngas-gasoline mixtures to be propagated much closer to the cylinder wall and crevices, which benefits improving the engine combustion efficiency and therefore elevating the engine indicated thermal efficiency.

3.3. *Combustion analysis*

Flame development (CA0-10) and propagation (CA10-90) periods directly reflect the engine combustion quality. CA0-10 is defined as the crank angle duration from the spark discharge to 10% heat release of the total fuel, and CA10-90 is defined as the crank angle duration from 10% to 90% heat release of the total fuel. Figs. 7 and 8 display the variations of CA0-10 and CA10-90 with syngas enrichment at 1800 rpm and a MAP of 61.5 kPa. It can be found from Figs. 7 and 8 that both CA0-10 and CA10-90 are shortened after the syngas blending. When the syngas volume fraction rises from 0% to 2.43%, CA0-10 and CA10-90 are shortened by about 6.2% and 4.5% compared with those of the original engine, respectively. This can be ascribed to the fact that as the ignition energies of hydrogen and carbon monoxide are lower than that of gasoline, the syngas can be ignited much more easily than the pure gasoline. Moreover, the hydrogen in the syngas helps stimulate the formation of O and OH radicals which avail enhancing and accelerating the chain reaction in the fuel combustion process [48]. Since

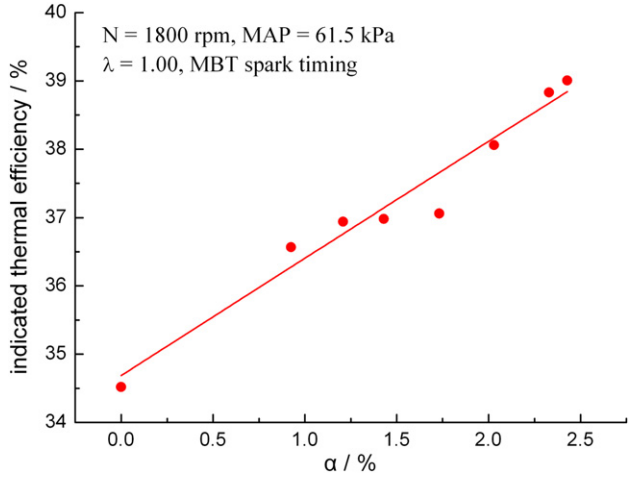

Fig. 6 – Indicated thermal efficiency versus the syngas volume fraction at 1800 rpm and a MAP of 61.5 kPa.

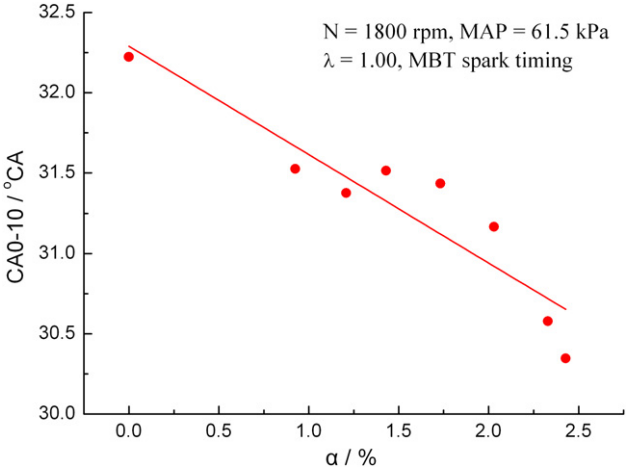

Fig. 7 – CA0-10 versus the syngas volume fraction at 1800 rpm and a MAP of 61.5 kPa.

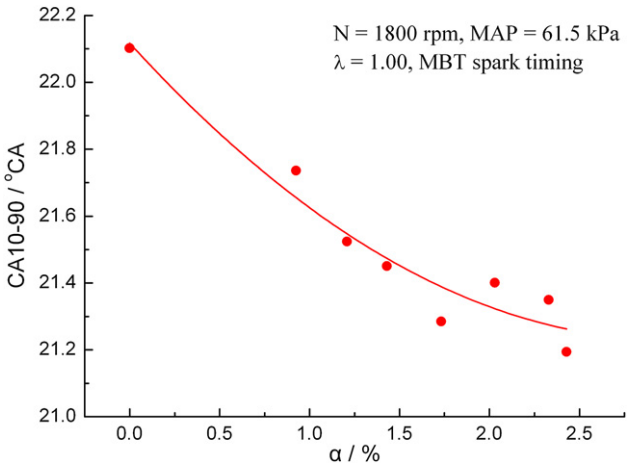

Fig. 8 – CA10-90 versus syngas volume fraction at 1800 rpm and a MAP of 61.5 kPa.

hydrogen and carbon monoxide possess higher burning velocity than gasoline, the flame of the syngas-gasoline mixtures can be propagated more quickly than that of pure gasoline. Therefore, both CA0-10 and CA10-90 are obviously reduced with the increase of syngas volume fraction.

3.4. *Exhaust emissions*

In this section, HC, CO, and NOx emissions before a three-way catalytic converter are measured to investigate the effect of syngas addition on the engine emissions characteristics. Fig. 9 shows HC emissions against syngas volume fraction at 1800 rpm and a MAP of 61.5 kPa. It can be found from Fig. 9 that HC emissions are effectively reduced with the increase of syngas blending ratio. When the syngas volume fraction in the total intake gas reaches the maximum value of 2.43%, HC emissions from the syngas-blended gasoline engine are about 15.47% lower than those from the original engine. This can be attributed to the fact that, for a specified excess air ratio, the decreased gasoline flow rate is attained with the syngas enrichment, causing the decreased source of HC emissions. Meanwhile, the high flame and diffusion speeds of syngas benefit the complete combustion of mixtures in cylinder. Therefore, HC emissions are distinctly reduced with the increase of syngas blending level.

As it is shown in Fig. 10, CO emission increases with the increase of syngas addition level. It can be seen from Fig. 10 that CO emission raises to 3821 ppm when syngas volume fraction achieves to 2.43%. The possible reason is that the combustion of hydrogen consumes more O_2 due to the high stoichiometric air-to-fuel ratio of hydrogen. Furthermore, the high flame speed of hydrogen also indicates that the combustion of hydrogen could consume more adjacent air to cause some lean oxygen areas where CO can be quickly formed. Besides, with the increase of syngas blending ratio, the ethanol concentration in the syngas is unexpectedly increased. The evaporation of ethanol has to consume energy, and therefore reduces the cylinder temperature. Thus, the shortened combustion duration and reduced combustion temperature decrease the time and temperature required for the CO oxidation. Moreover, the carbon monoxide in the syngas may also be ascribed to be a reason for the increased CO emission after the syngas addition. Since the fresh air is gradually removed with the increase of syngas enrichment level, the decreased O_2 concentration in the total intake gas also blocks CO to be fully converted into CO_2.

Fig. 11 depicts NOx emissions versus syngas volume fraction at 1800 rpm and a MAP of 61.5 kPa. As it is shown in Fig. 11, NOx emissions are generally decreased with the increase of syngas blending ratio. When the syngas volume fraction rises from 0% to 2.43%, NOx emissions are reduced by 15.47%. Since the volume energy densities of hydrogen and carbon monoxide are lower than that of gasoline, the total fuel energy flow rate is decreased with the increase of syngas addition fraction at a specified excess air ratio. Moreover, the evaporation of ethanol at high syngas flow rates also consumes energy and therefore reduces the cylinder temperature. As a result, NOx emissions are decreased with the increase of syngas addition fraction, due to the dropped cylinder temperature.

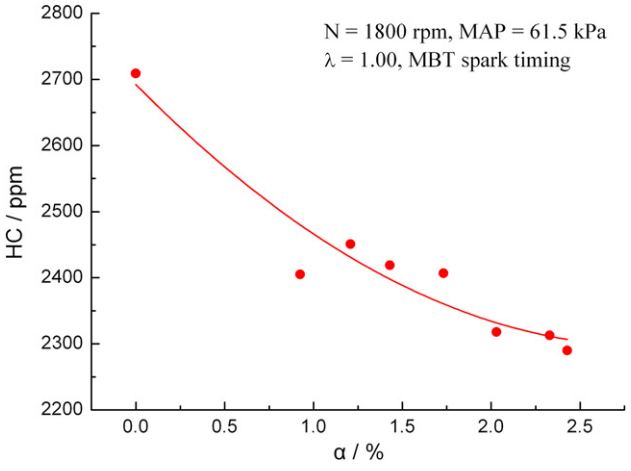

Fig. 9 – HC versus the syngas volume fraction at 1800 rpm and a MAP of 61.5 kPa.

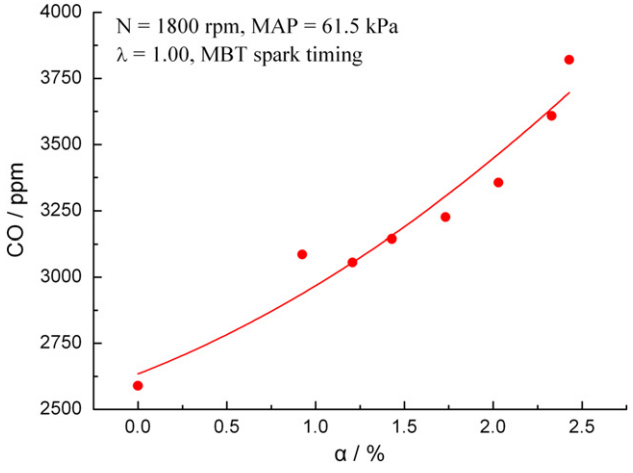

Fig. 10 – CO versus the syngas volume fraction at 1800 rpm and a MAP of 61.5 kPa.

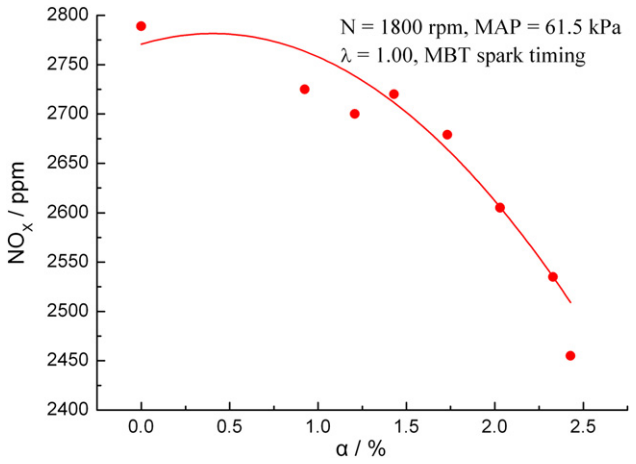

Fig. 11 – NOx versus syngas volume fraction at 1800 rpm and a MAP of 61.5 kPa.

4. Conclusions

This paper investigated the combustion and emissions characteristics of an SI engine fueled with the syngas-gasoline blends. A reforming reactor covered with copper based catalysts was used to produce the syngas with the engine exhaust heat. The main conclusions are listed as follows:

1. The syngas flow rate and ethanol conversion efficiency are markedly enhanced with the increase of the feedstock flow rate. There is an inverse relation between hydrogen and carbon monoxide concentrations in the syngas with the increase of the feedstock flow rate.
2. The reduced fuel energy flow rate results in the dropped Imep at high syngas volume fractions in the intake gas. Because of the enhanced combustion process after the syngas enrichment, the engine indicated thermal efficiency is heightened from 34.52% of the original engine to 39.01% of the 2.43% syngas-blended gasoline engine.
3. Since the low ignition energies and high flame speeds of hydrogen and carbon monoxide in the syngas permit the syngas-gasoline mixtures to be easily ignited and quickly combusted, both CA0-10 and CA10-90 are shortened with the increase of syngas blending fraction.
4. HC and NOx emissions are decreased with the increase of syngas volume fraction. But CO emission is increased with syngas addition, due to the reduced cylinder temperature.

Acknowledgments

This work was supported by Key Program of Sci & Tech Project of Beijing Municipal Commission of Education (Grant No. KZ201210005002), Ph.D. Programs Foundation of Ministry of Education of China (Grant No. 20111103110010) and Beijing Municipal Natural Science Foundation (Grant No. 3122006). The authors also appreciate all students in the group for their help with the experiment.

REFERENCES

[1] Veziroglu TN, Barbir F. Hydrogen, the wonder fuel. Int J Hydrogen Energy 1992;17:391–404.
[2] Ma F, Wang M, Jiang L, Chen R, Deng J, Naeve N, et al. Performance and emission characteristics of a turbocharged CNG engine fueled by hydrogen-enriched compressed natural gas with high hydrogen ratio. Int J Hydrogen Energy 2010;35:6438–47.
[3] Ma F, Wang M. Performance and emission characteristics of a turbocharged spark-ignition hydrogen-enriched compressed natural gas engine under wide open. Int J Hydrogen Energy 2010;35:12502–9.
[4] Ma F, Wang Y, Ding S, Jiang L. Twenty percent hydrogen-enriched natural gas transient performance research. Int J Hydrogen Energy 2009;34:6523–31.
[5] Fischer HC, Brereton GJ. Fuel injection strategies to minimize cold-start HC emission. In: SAE paper no. 1997-02-24; 1997.
[6] Ma F, Ding S, Wang Y, Wang M, Jiang L, Naeve N, et al. Performance an emission characteristics of a Spark-Ignition (SI) Hydrogen-enriched compressed natural gas (HCNG) engine under various operating conditions including idle conditions. Energy Fuels 2009; 23:3113–8.
[7] Al-Janabi HAKS, Al-Baghdadi MARS. A prediction study of the effect of hydrogen blending on the performance and pollutants emission of a four stroke spark ignition engine. Int J Hydrogen Energy 1999;24:363–75.
[8] Ma F, Liu H, Wang Y, Li Y, Wang J, Zhao S. Combustion and emission characteristics of a port-injection HCNG engine under various ignition timings. Int J Hydrogen Energy 2008; 33:816–22.
[9] Ma F, Wang Y, Liu H, Li Y, Wang J, Ding S. Effects of hydrogen addition on cycle-by-cycle variations in a lean burn natural gas spark-ignition engines. Int J Hydrogen Energy 2008;33: 823–31.
[10] Ji C, Wang S. Combustion and emissions performance of a hybrid hydrogen–gasoline engine at idle and lean conditions. Int J Hydrogen Energy 2010;35:346–55.
[11] Ji C, Wang S, Zhang B. Effect of spark timing on the performance of a hybrid hydrogen–gasoline engine at lean conditions. Int J Hydrogen Energy 2010;35:2003–12.
[12] Ma F, Wang J, Wang Y, Wang Y, Li Y, Liu H, et al. Influence of different volume percent hydrogen/natural gas mixtures on idle performance of a CNG engine. Energy Fuels 2008;22: 1880–7.
[13] Ji C, Wang S. Experimental study on combustion and emissions performance of a hybrid hydrogen–gasoline engine at lean burn limits. Int J Hydrogen Energy 2010;35: 1453–62.
[14] Ma F, Wang Y, Wang M, Liu H, Wang J, Ding S, et al. Development and validation of a quasi-dimensional combustion model for SI engine fuelled by HCNG with variable hydrogen frctions. Int J Hydrogen Energy 2008;33: 4863–75.
[15] Ji C, Wang S, Zhang M, Zhang B. Reducing the idle speed of a spark-ignited gasoline engine with hydrogen addition. Int J Hydrogen Energy 2010;35:10580–8.
[16] Salimi F, Shamekhi AH, Pourkhesalian AM. Role of mixture richness, spark and valve timing in hydrogen-fueled engine performance and emission. Int J Hydrogen Energy 2009;34: 3922–9.
[17] Ma F, Wang Y, Liu H, Li Y, Wang J, Zhao S. Experimental study on thermal efficiency and Emission characteristics of a lean burn hydrogen enriched natural gas engine. Int J Hydrogen Energy 2007;32:5067–75.

[18] Ma F, Wang Y. Study on the extension of lean operation limit through hydrogen enrichment in a natural gas spark-ignition engine. Int J Hydrogen Energy 2008;33:1416–24.
[19] Das LM. Hydrogen-oxygen reaction mechanism and its implication to hydrogen engine combustion. Int J Hydrogen Energy 1996;21:703–15.
[20] Ganeshb RH, Subramaniana V, Balasubramanianb V, Mallikarjuna JM, Ramesh A, Sharma RP. Hydrogen fueled spark ignition engine with electronically controlled manifold injection: an experimental study. Renewable Energy 2008;33: 1324–33.
[21] Akansu SO, Kahraman N, Ceper B. Experimental study on a spark ignition engine fuelled by methane-hydrogen mixtures. Int J Hydrogen Energy 2007;32:4279–84.
[22] Al-Baghdadi MARS. Performance study of a four-stroke spark ignition engine working with both of hydrogen and ethyl alcohol as supplementary fuel. Int J Hydrogen Energy 2000; 25:1005–9.
[23] Liu B, Huang Z, Zeng K, Chen H, Wang X, Miao H, et al. Experimental study on emissions of a spark-ignition engine fueled with natural gas hydrogen blends. Energy Fuels 2008; 22:273–7.
[24] Yousufuddin S, Mehdi SN, Masood M. Performance and combustion characteristics of a hydrogen ethanol-fuelled engine. Energy Fuels 2008;22:3355–62.
[25] Ji C, Wang S. Effect of hydrogen addition on the idle performance of a spark ignited gasoline engine at stoichiometric condition. Int J Hydrogen Energy 2009;34: 3546–56.
[26] Ji C, Wang S. Effect of hydrogen addition on combustion and emissions performance of a spark ignited gasoline engine at lean conditions. Int J Hydrogen Energy 2009;34:7823–34.
[27] Ji C, Wang S. Combustion and emissions characteristics of a hybrid hydrogen-gasoline engine under various loads and lean conditions. Int J Hydrogen Energy 2010;35:5714–22.
[28] Wang S, Ji C, Zhang B. Effect of hydrogen addition on combustion and emissions performance of a spark-ignited ethanol engine at idle and stoichiometric conditions. Int J Hydrogen Energy 2010;35:9205–13.
[29] Li J, Guo L, Du T. Formation and restraint of toxic emissions in hydrogen-gasoline mixture fueled engines. Int J Hydrogen Energy 1998;23:971–5.
[30] Profeti LPR, Ticianelli EA, Assaf EM. Production of hydrogen by ethanol steam reforming on Co/Al2O3 catalysts: effect of addition of small quantities of noble metals. J Power Sources 2008;175:482–9.
[31] Dunn S. Hydrogen futures: toward a sustainable energy system. Int J Hydrogen Energy 2002;27:235–64.
[32] Heracleous E. Well-to-Wheels analysis of hydrogen production from bio-oil reforming for use in internal combustion engines. Int J Hydrogen Energy 2011;36: 11501–11.
[33] Shudo T, Shima Y, Fujii T. Production of dimethyl ether and hydrogen by methanol reforming for an HCCI engine system with waste heat recovery-Continuous control of fuel ignitability and utilization of exhaust gas heat. Int J Hydrogen Energy 2009;34:7638–47.
[34] Talom HL, Beyene A. Heat recovery from automotive engine. Appl Therm Eng 2009;29:439–44.
[35] Arias DA, Shedd TA, Jester RK. Theoretical analysis of waste heat recovery from an internal combustion engine in a hybrid vehicle; 2006. In: SAE paper no. 2006-01-1605.
[36] Teng H, Regner G, Cowland C. Achieving high engine efficiency for heavy-duty diesel engines by waste heat recovery using supercritical organic-fluid rankine cycle; 2006. In: SAE paper 2006-01-3522.
[37] Heywood J. Internal combustion engine fundamentals. New York: McGraw Hill; 1988.
[38] Raju ASK, Park CS, Norbeck JM. Synthesis gas production using steam hydrogasification and steam reforming. Fuel Process Technol 2009;90:330–6.
[39] Peppley BA, Amphlett JC, Kearns LM, Mann RF. Methanol-steam reforming on Cu/ZnO/Al2O3. Part 1: the reaction network. Appl Catal. A 1999;179:21–9.
[40] Koh ACW, Chen L, Leong WK, Ang TP, Johnson BFG, Khimyak T, et al. Ethanol steam reforming over supported ruthenium and ruthenium-platinum catalysts: comparison of organometallic clusters and inorganic salts as catalyst precursors. Int J Hydrogen Energy 2009;34:5691–703.
[41] Liguras DK, Kondarides DI, Verykios XE. Production of hydrogen for fuel cells by steam reforming of ethanol over supported noble metal catalysts. Appl Catal. B 2003;43: 345–54.
[42] Llorca J, Homs N, Sales J, Piscina PR. Efficient production of hydrogen over supported cobalt catalysts from ethanol steam reforming. J Catal 2002;209:306–17.
[43] Yang Y, Ma J, Wu F. Production of hydrogen by steam reforming of ethanol over a Ni/ZnO catalyst. Int J Hydrogen Energy 2006;31:877–82.
[44] Huang G, Liaw BJ, Jhang CJ, Chen YZ. Steam reforming of methanol over CuO/ZnO/CeO2/ZrO2/Al2O3 catalysts. Appl Catal. A 2009;358:7–12.
[45] Park C, Choi Y, Kim C, Oh S, Lim G, Moriyoshi Y. The performance and exhaust emission characteristics of a spark ignition engine using ethanol and ethanol-reformed gas. Fuel 2010;89:2118–25.
[46] Biniwale RB, Ichikawa NKM. Production of hydrogen-rich gas via reforming of iso-octane over Ni-Mn and Rh-Ce bimetallic catalysts using spray pulsed reactor. Catal Lett 2005;100: 17–25.
[47] Profeti LPR, Dias JAC, Assaf JM, Assaf EM. Hydrogen production by steam reforming of ethanol over Ni-based catalysts promoted with noble metals. J Power Sources 2009; 190:525–33.
[48] Conte E, Boulouchos K. Influence of hydrogen-rich-gas addition on combustion, pollutant formation and efficiency of an IC-SI engine; 2004. In: SAE paper No.2004-01-0972.

Nomenclature

SR: steam reforming
SRE: steam reforming of ethanol
SRM: steam reforming of methanol
WGSR: water gas shift reaction
GC: gas chromatograph
TCD: thermal conduct detector
OECU: original electronic control unit
HECU: hybrid electronic control unit
CA: crank angle
MAP: manifolds absolute pressure
MBT: maximum brake torque
Imep: indicated mean effective pressure (bar)
α: syngas volume fraction in the total intake gas (%)
λ: global excess air ratio
$\dot{v}_s$: volumetric flow rate of syngas (L/h)
$\dot{v}_{air}$: volumetric flow rate of air (L/h)
$\dot{m}_{air}$: mass flow rate of air (g/min)
$\dot{m}_g$: mass flow rate of gasoline (g/min)
$\dot{m}_{H_2}$: mass flow rate of hydrogen (g/min)
$\dot{m}_{CO}$: mass flow rate of carbon monoxide (g/min)
$AF_{st,g}$: stoichiometric air-to-fuel ratio of gasoline
AF_{st,H_2}: stoichiometric air-to-fuel ratio of hydrogen
$AF_{st,CO}$: stoichiometric air-to-fuel ratio of carbon monoxide
CA0-10 CA: duration of 0–10% heat release (°CA)
CA10-90 CA: duration of 10%–90% heat release (°CA)